Evaluating the performance of fibrillar collagen films formed at polystyrene surfaces as cell culture substrates

John T. Elliott,[a] Michael Halter, and Anne L. Plant
Cell and Tissue Measurements Group, Chemical Science and Technology Laboratory, National Institute of Standards and Technology, Gaithersburg, Maryland 20899

John T. Woodward
Physics Laboratory, National Institute of Standards and Technology, Gaithersburg, Maryland 20899

Kurt J. Langenbach
American Type Culture Collection, Manassas, Virginia 20108

Alessandro Tona
Scientific Applications International Corp. (SAIC), Alexandria, Virginia 22314

(Received 23 January 2008; accepted 1 April 2008; published 30 April 2008)

While it is well-appreciated that the extracellular matrix plays a critical role in influencing cell responses, well-defined and reproducible presentation of extracellular matrix proteins poses a challenge for *in vitro* experiments. Films of type 1 collagen fibrils assembled on alkanethiolate monolayers formed at gold-coated surfaces have been shown to elicit a cellular response comparable to collagen gels, but with the advantages of excellent optical properties, and high reproducibility and robustness. To make this collagen matrix more accessible to laboratories that do not have access to gold film deposition the authors have examined the use of untreated polystyrene as a substrate for forming fibrillar collagen films. Direct comparison of films of fibrillar collagen fibrils formed at polystyrene with those formed at alkanethiolate monolayers indicates that films of collagen formed on these two surfaces compare very favorably to one another, both in their supramolecular structural characteristics as well as in the cell response that they elicit. Both substrates exhibit a dense covering of fibrils approximately 200 nm in diameter. The spreading of fibroblasts and activation of the tenascin-C gene promoter are statistically equivalent as determined by a metric derived from the *D*-statistic normally used in the Kolmogorov-Smirnov statistical test. The results of this study suggest that biologically relevant, robust thin films of collagen fibrils can be formed in any laboratory in untreated polystyrene dishes and multi-well polystyrene plates. © *2008 American Vacuum Society.* [DOI: 10.1116/1.2912936]

I. INTRODUCTION

Type I collagen is the most prevalent protein in the body. It is synthesized as a triple helical monomeric unit that polymerizes outside of cells to form supramolecular fibrillar structures. Collagen fibrils serve as a critical component of ligaments, tendons, and bone, as well as the primary extracellular matrix (ECM) for soft tissues such as skin and liver.[1] Most cells in the body are associated with a matrix containing collagen. Collagen is an important matrix for tissue engineering applications[2,3] and is a frequent subject in the study of the effect of extracellular matrix modifications and mechanical influences of extracellular matrix on wound healing,[4] vascular disease,[5,6] and growth and proliferation of normal and cancer cells.[7,8]

An important experimental system for mimicking the *in vivo* collagen matrix consists of gels of type 1 collagen prepared by allowing collagen monomers in solution to polymerize into a network of fibrils. While this is a well-accepted and useful experimental tool, collagen gels have some disadvantages. They are fragile structures that are often altered or destroyed during routine handling procedures (e.g., solution addition and removal). Their thickness (millimeters) results in substantial light scattering and therefore reduces the image quality of cells observed with light microscopy. They can trap fluorescent molecules used to label cell constituents and add to fluorescence background signal. Importantly, their properties are difficult to quantify by analytical methods; inconsistencies in density, thickness, and integrity are difficult to assess, and the degree of reproducibility even in gels prepared under identical conditions cannot be quantitatively determined.

We have shown in previous reports that type 1 collagen polymerizes and self assembles into a layer of fibrils at the surface of alkanethiolate monolayers.[9] Thiolate monolayers have frequently been used to produce a highly ordered chemically modified surface coating to allow adsorption of ECM proteins such as fibronectin.[10] Our studies with collagen have shown than at a hydrophobic alkanethiol interface, a network of collagen fibrils forms a thin film with an effective medium thickness on the order of 40 nm. Larger fibrils 200 nm in diameter and tens of microns in length carpet the surface and appear to grow out of smaller fibrils about 25 nm in diameter that are in intimate contact with the alkanethiolate monolayer.[9] We have shown by ellipsometry

[a]Electronic mail: jelliott@nist.gov

and atomic force microscopy (AFM) that thin films of collagen can be formed reproducibly,[9] and that the supramolecular structure of fibrils can be tuned by altering the solution concentration of collagen[9] or the chemistry of the alkylthiolate surface.[11] We have shown that cells are sensitive to the density of large fibrils[9] and to the mechanical properties[12] and orientation[13] of collagen fibrils. Furthermore, films of collagen fibrils are easy to form and are highly robust under handling conditions such as multiple washing steps and transporting large distances. They are spatially homogeneous, ensuring a consistent cellular response within an experiment. Because they are formed on gold-coated glass slides or silicon wafer, they can be examined by a number of analytical techniques. They can be formed on semitransparent films of gold (approximately 6 nm in thickness), and cells growing on these surfaces are readily visible by transmission and epifluorescence microscopy. Because the films of collagen are so thin, their optical properties facilitate high resolution visualization of the interactions of cells with individual collagen fibrils.[12]

Cells on films of collagen fibrils display many of the characteristics associated with cells in a three-dimensional matrix. We have observed that A10 vascular smooth muscle cells will reorganize the collagen fibrils and bury themselves under fibrils during several hours in culture.[12] We have demonstrated that vascular smooth muscle cells and NIH 3T3 fibroblasts respond to films of collagen in a manner that is apparently identical to their response to thick gels of collagen by examining integrin engagement, proliferation rates, gene expression, ERK phosphorylation, morphology, and cytoskeletal organization.[14,15] Such data can provide mechanistic understanding of cell response to collagen in tissue and scaffolding, and how cell response to other environmental factors is influenced by ECM conditions.

Although alkanethiol self-assembled monolayer technology is robust and well-established,[10] many labs do not have easy access to deposition of thin layers of precious metals onto substrates as is required for the use of alkanethiol monolayers. The approach is also difficult to employ in common applications that use plastic and multi-well culture plates. Because of the difficulty of preparing physiologically relevant matrices, many research studies are carried out on poorly defined ECM matrices that are difficult to characterize and reproduce. Specialized applications such as automated microscopy and high content screening are often carried out on surfaces that have little in common with physiological conditions, such as tissue culture polystyrene (TCPS). While TCPS is likely adsorptive to adhesive serum proteins, it is difficult to characterize the composition and structure of those adsorbed proteins. In an effort to make fibrillar collagen films accessible to more laboratories, we evaluated alternative substrates for formation of collagen fibrils. In a study of the influence of surface free energy on the formation of thin films of collagen fibrils, we examined collagen interaction with alkylthiolate monolayers having different terminal functional groups.[11] We found that formation of complete and stable fibrillar films of collagen requires a hydrophobic surface with a contact angle with water that was greater than approximately 80°, The contact angle of untreated polystyrene (PS) that has not had surface chemistry modifications to enhance cell adhesion is about 90°, suggesting that untreated PS may be a surface at which fibrils of type 1 collagen may form.

In this report, we demonstrate the use of PS as a substrate for forming films of collagen fibrils, and compare fibrillar collagen films formed on PS dishes with fibrillar collagen films formed at alkanethiol monolayers. We find that films of fibrillar collagen formed on these two surfaces compare very favorably to one another, both in their physical characteristics as well as in the response that they elicit in NIH 3T3 fibroblast cells. The statistical comparison of the cell populations on the different substrates was achieved with a metric derived from the *D*-statistic normally used in the Kolmogorov-Smirnov statistical test. This nonparametric test takes into account the *between-treatment* and *within-treatment* variations in the distribution of cell responses measured on the substrate preparations. The results of this study suggest that robust, reproducible thin films of collagen fibrils, with excellent optical properties and ease of handling, can be formed in any laboratory in untreated polystyrene dishes.

II. METHODS AND MATERIALS

Commercial names of materials and apparatus used during this study are identified only to specify the experimental procedures. This does not imply a recommendation by NIST, nor does it imply that they are the best available for the purpose. The accepted SI unit of concentration, mol/L, has been represented by the symbol M in order to conform to the conventions of this journal.

A. Alkanethiolate monolayer films

Semitransparent gold films (6 nm thick, for atomic force and optical microscopy) on glass coverslips were prepared as described previously.[9] 1-Hexadecanethiol (Aldrich, St. Louis MO), as a 0.5 mM solution in 99.5% ethanol (Aldrich), was allowed to adsorb to gold films by incubating gold surfaces directly in the thiol solution for 16 h. These substrates were rinsed with ethanol and dried with 0.02 μm pore size filtered N_2 prior to incubation with collagen solution.

B. Formation of collagen films

This procedure has been described previously.[9,11] Dried thiol-covered gold-coated coverslips were placed in six-well polystyrene culture plates (BD, Franklin, NY). A collagen solution at $\sim$3 mg/mL (PureCol, Nutacon, Leimuiden, The Netherlands) was neutralized with tenfold concentrated Dulbecco's phosphate buffer (PBS) and 0.1 N NaOH in a final dilution ratio of 8:1:1 volume fraction. The collagen solution was diluted with PBS (7:1 volume fraction) and poured over the individual gold-coated substrates. The final concentration of collagen was 320 μg/mL and 3 mL of collagen solution was used for each substrate. A sufficiently high concentration

and volume of collagen must be used or the collagen will fail to form a bed of large fibrils, which is essential for the physiologically relevant response. The six-well plates were placed in a hydrated incubator at 37 °C for greater than 16 h. The coverslips were lifted out of the collagen solution so the bulk collagen gel slid off the surface. The collagen-coated coverslips were rinsed extensively with PBS and then H_2O from Teflon squirt bottles (Fisher Scientific, Pittsburgh, PA) to remove residual bulk collagen gel, dried for approximately 20 s with 0.02 μm pore size filtered N_2, and placed back into PBS in six-well culture plates and stored at 4 °C until use. All steps were performed under sterile conditions.

A similar procedure was used to assemble collagen fibrils at untreated polystyrene surfaces. Untreated polystyrene six-well plates (BD, Franklin Lakes, NJ) were filled with 3 mL of the collagen solution prepared by dilution as described above and incubated at 37 °C for at least 16 h. The plate was set on an angle against the edge and floor of a sterile plastic tray and the bulk collagen solution was removed from the wells by aspiration. Each well was rinsed with PBS and then H_2O from Teflon squirt bottles, dried for approximately 20 s with 0.02 μm pore size filtered N_2, and PBS was added to each well. The plate was stored at 4 °C until use.

Prior to plating cells, the collagen-coated substrates were pre-equilibrated with 10%(v/v) fetal bovine serum in Dulbecco's modified Eagle medium (10% FBS/DMEM) for 3 h at 37 °C.

C. Atomic force microscopy (AFM) and phase imaging of substrates

Collagen films and untreated polystyrene (PS) in the absence of collagen were imaged in air with a PicoScan AFM instrument (Molecular Imaging, AZ) in intermittent contact mode as previously described.[9] Phase microscopy images were collected through a 20× objective on a Zeiss Axiovert 100 inverted microscope. Collagen-coated gold coverslip or polystyrene was rinsed with ultra-purified H_2O (Millipore, Billerica, MA) and dried with filtered N_2. The dry gold coverslip was directly inverted onto a glass coverslide for imaging. A portion of the dry PS substrate was cut from the well bottom with a hand-held Dremel tool and directly inverted onto a glass coverslide for imaging.

D. Cell culture, fixation, and staining

NIH 3T3 fibroblasts were acquired from American Type Culture Collection (Manassas, VA). A stable reporter cell line was produced by transfection with a construct containing the full-length tenascin-C promoter region linked to the gene for destabilized EGFP (dsEGFP).[15] The cell line resulting from transfection with this TN-C-dsEGFP construct was maintained in 10% FBS/DMEM, passaged on a 4/5-day culturing cycle, and used before passage 29. For experiments, cells were trypsinized, counted, rinsed, and resuspended in 10% FBS/DMEM. The cells were seeded on the substrates at 800–1000 cells/cm^2, which minimizes cell-cell contact and facilitates automated edge detection with image analysis software. Cells were incubated for 24 h on substrates and fixed with N-maleimidobenzoyl-N-hydroxysuccinimide ester (10 mg/mL fresh stock in DMSO, 1 mg/mL final concentration, Sigma-Aldrich) in a microtubule stabilizing buffer [4%(w/v) polyethylene glycol 8000, 100 mM PIPES, 1 mM EGTA, *p*H 6.9] for 16 h as described previously.[15] This fixative preserves the soluble GFP concentration within the cells.

For staining, fixed cells were permeabilized with 0.02% Tx-100 and stained with Texas-Red-C_2-maleimide [TxRed, 5 mg/mL stock in dimethylformamide (DMF), 10 ng/mL final concentration, Invitrogen] and 4′,6-diamidino-2-phenylindole (DAPI, 1 mg/mL stock in DMF, 2 ng/mL final concentration) as previously described.[15] The staining concentrations were optimized to the highest concentration of stain that does not exhibit significant emission through the filters used to image GFP during the expected exposure time. This alleviates the need to use a compensation matrix to adjust image intensities for dye bleed through. The stained cells were rinsed with PBS, 3% BSA in PBS and PBS containing 0.05% NaN_3 (Sigma-Aldrich). Mounting solution (3 mL) composed of 50%(v/v) glycerol in 10 mM Tris, *p*H 8.0, and 0.9 g/L 1,4-diazobicyclo[2,2,2]octane (DABCO) to reduce photobleaching was added to cells in the six-well plates. Cells on a glass coverslip in the same mounting solution were lifted from a well and, without draining, were inverted onto thin glass coverslides. The coverslip was clipped to the coverslide with small alligator clips and the excess mounting media on the coverslip surface was rinsed off with a stream of ultra-purified H_2O. The excess water was removed by tapping on a paper towel and blowing it dry with a stream of air. This mounting procedure optimized the optical quality of the mounted coverslips. These samples were directly imaged through the coverslide on the optical microscope. Each experiment was performed in triplicate.

E. Automated fluorescence microscopy

Imaging was performed with an Axiovert 100 inverted fluorescent microscope (Carl Zeiss, Inc.) fitted with a computer-controlled automated stage, excitation and emission color filter wheels (Ludl, Hawthorne, NJ), dichroic beamsplitter, phase microscopy optics, a 100 W mercury arc lamp, and CCD camera (CoolSnap FX, Roper Scientific, Tucson, AZ). The specifications for the fluorescent filters were as follows: (1) a custom dichroic multipass beam splitter optimized for imaging DAPI, EGFP, and TxRed (part # BS51019+400dclp, Chroma Technology, VT); (2) DAPI excitation filter, 360/40 nm; (3) DAPI emission filter, 460/50 nm; (4) EGFP excitation filter, 470/40 nm; (5) EGFP emission filter, 525/50 nm; (6) TxRed excitation filter, 568/24 nm; and (7) TxRed emission filter, 630/60 nm. A computer software routine (ISee Imaging Systems, Raleigh, NC) moves the stage to a position, autofocuses on the field based on the intensity variance of the TxRed stain, and then collects four images of the same field of cells. These four images are a phase contrast image and three fluorescence images at appropriate filter settings for TxRed, GFP, and DAPI.[15,16] Approximately 100 fields (containing a total of 300–1000 cells) were sampled on each substrate.

To confirm that lamp intensity did not change appreciably during the course of any of the measurements, lamp intensity was monitored at several points during experiments using photostable fluorescent glass (Schott GG475, Edmund Optics, Barrington, NJ) under the GFP imaging conditions.[16] Flat field correction under the GFP imaging conditions was achieved by minimizing the fluorescent intensity variations across the imaging field of the CCD camera to less than 3% CV by optimizing lamp focusing and alignment on the photostable fluorescent glass.

F. Normalization of fluorescent intensities between substrates

The differences in optical properties between the gold-coated coverslips and the polystyrene wells required normalizing the measured cellular GFP fluorescence to compensate for differences in adsorption and reflection of excitation and emission light. To achieve this, a calibration kit consisting of 6 μm fluorescent beads with excitation and emission peaks at 505 and 515 nm, respectively (Invitrogen, Carlsbad CA), was used. An aliquot of the 0.3% relative intensity beads was collected by centrifugation, resuspended in ethanol, and a few drops were added to a representative gold substrate or the bottom of a well in a PS plate. As the ethanol evaporated, the beads were physisorbed to the surface and the samples could be treated identically to the corresponding samples containing cells. Automated microscopy, using the filters arrangement and exposure time identical to that used for imaging GFP in cells, was used to collect images of the fluorescent beads from 50 to 100 fields. An image analysis routine provided segmentation of every fluorescent object composed of single or multiple beads, and the maximum intensity and local background intensity around each object was determined. For analysis, we assumed the distribution of maximum bead intensities from each sample is drawn from the same distribution. The ratio of intensities measured from the different substrates provided a simple correction factor that was used to scale the intensity data from cells on the different substrates. The measured GFP intensities on the gold films prepared in this experiment were multiplied by a factor of 0.72 to normalize the intensities with those measured on the PS dishes.

G. Image analysis

Image analysis was performed using the open-source package, ImageJ (http://rsb.info.nih.gov/ij/) with custom plug-in routines. Segmentation of cells in the images involved empirically determining a threshold value to identify objects stained with TxRed. This segmentation operation was used to derive cell areas and to generate a cell-object mask for quantifying the cellular GFP intensity. A similar approach was used to identify nuclei in the images of DAPI stained cells. The number of nuclei per TxRed object was used to identify groups of cells, single cells, or debris. Only segmented objects with a single nucleus were considered for this analysis. Size discrimination filter routines were used to remove very large and very small objects from the data set that did not correspond to cells or nuclei. For GFP intensity determination, an average background intensity was determined from a 3 pixel ring around each cell. The total GFP intensity was determined by subtracting an average background intensity from each pixel within the segmented cell area.

H. Statistical analysis

Quantitative and statistical analyses of all data were performed with spreadsheet software (Excel, Microsoft). Cell area and GFP fluorescence intensity data sets were compared to one another by converting the cellular data from each experiment into a cumulative distribution. A macro routine adapted from a published algorithm[17] was used to generate cumulative distributions with a common X-axis scale from all measured area or fluorescence intensity values. For three replicate experiments, a mean cumulative distribution curve was generated by averaging the cumulative fraction value (Y-axis value) at each measured value (X-axis) of the cumulative distributions from the replicate curves. The standard deviation in the average cumulative fraction for each value in the X-axis was also calculated. The resulting plots can be seen in two separate figures in this work.

Using the plots of the mean cumulative distributions, the maximum absolute vertical difference between any two curves was determined and used as the metric for the difference between the two compared distributions (for example, see Ref. 18). This difference metric is identical to the test statistic (called the D-statistic) used for the Kolmogorov-Smirnov statistical test.[17] Thus, at every value on the X-axis the absolute difference between corresponding Y-axis values was determined, and the maximum difference, the D-statistic, was taken as a measure of the difference between two curves. This value was treated as the *between-treatment* D-statistic value.

To determine statistical significance of the differences between treatments, the *between-treatment* D-statistic values were comparing *within-treatment* D-statistic values. We define a test statistic as the ratio of the *between-treatment* variation to the *within treatment* variation according to Eq. (1),

$$\text{Test statistic ratio} = \frac{D_{\text{between-treatments}}}{\sqrt{(SE_a)^2 + (SE_b)^2}}, \tag{1}$$

where $D_{\text{between-treatments}}$ is the D-statistic between mean cumulative distributions, and the combined standard error in the denominator is determined from

$$SE_a = \frac{\sqrt{\sum_{i=1}^{i=N} (D_{ai})^2}}{N_a - 1} \tag{2a}$$

for treatment a, and

$$SE_b = \frac{\sqrt{\sum_{i=1}^{i=N} (D_{bi})^2}}{N_b - 1} \quad (2b)$$

for treatment b, where D_i is the D-statistic calculated between each replicate cumulative distribution and its corresponding mean distribution curve, and N is the number of replicates per treatment ($N=3$ for this study). These formulas are similar to that used to determine the standard error in a mean from replicate data.

We consider two treatments to be statistically different from one another when the magnitude of the *between-treatment D*-statistic is a factor of 3 larger than the combined standard errors of the two treatments calculated from the *within-treatment D*-statistics. This will occur when the test statistic ratio in Eq. (1) is larger than 3. The use of 3 as the threshold value for determining statistical significance in this test can be considered similar to the use of 3 (i.e., 3 standard deviations) as a threshold value for statistical significance when comparing mean values.

III. RESULTS

A. Analysis of collagen films

We previously showed that surface free energy mediates fibrillar collagen film formation,[11] and suggested that the hydrophobicity of untreated PS may be sufficient to support collagen fibril organization. In this study, we directly compare fibrillar collagen films prepared on untreated PS to fibrillar collagen films formed on alkanethiolate monolayers. Figure 1 shows that collagen fibrils assembled at PS are very similar to collagen fibrils assembled at alkanethiolate monolayers. Collagen fibrils can be easily observed in phase contrast microscopy with a 10× or 20× objective lens. Optical microscopy [Figs. 1(a) and 1(b)] and AFM [Figs. 1(c)–1(f)] images are consistent with previously published images of collagen fibrils formed at alkanethiolate monolayers.[9,11,14] These images indicate that both PS and alkanethiolate monolayers support the formation of the supramolecular fibrillar structure of type 1 collagen and that these fibrils appear to be randomly distributed across both surfaces. The phase images show that the density of the fibrils on both the alkanethiolate monolayer and PS surface are similar. Higher resolution AFM images [Figs. 1(e) and 1(f)] show the presence of fibrils ranging in diameter from ~25 to 100 nm that appear to form adjacent to both the alkanethiolate surface and the PS surface in addition to the prominent 200 nm diameter fibrils. In the absence of collagen, the PS used in this study has a relatively smooth surface as indicated by AFM [Fig. 1(g)], with some apparent shallow scratches, but devoid of the features associated with the collagen.

B. Cellular response to collagen films

Previous studies have directly compared the response of NIH 3T3 fibroblasts and A10 vascular smooth muscle cells to thin films of collagen and to collagen gels.[9,14,15] A number

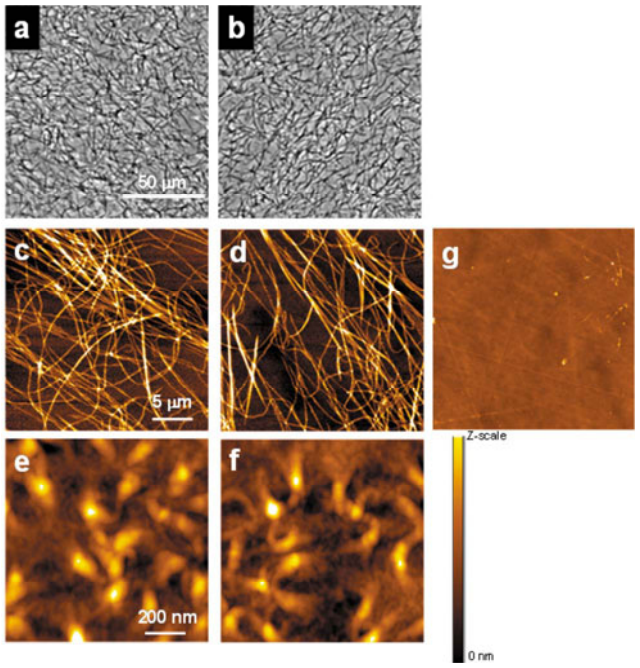

FIG. 1. Comparison of collagen supramolecular structure on different substrates. Optical microscopy of collagen fibrils assembled at an (a) alkanethiolate monolayer and (b) PS. AFM at a scan area of 25×25 μm^2 of collagen fibrils assembled at (c) an alkanethiolate monolayer or (d) PS; Z scale=0 −50 nm. AFM at a scan area of 1×1 μm^2 of collagen fibrils assembled at (e) an alkanethiolate monolayer or (f) PS; Z scale=0−3 nm. (g) AFM at a scan area of 25×25 μm^2 of untreated PS in the absence of collagen; Z =0−3 nm.

of criteria have been examined and were found to be apparently identical or nearly identical, including integrin ligation by cells with the collagen, cellular morphology, activation of the promoter for the ECM protein tenascin-C (TN-C) or expression of TN-C directly, cytoskeleton organization, and proliferation rate. In this study, we compare NIH 3T3 response to films of collagen formed on PS to those formed on alkanethiolate monolayers by comparing cell morphology and expression of GFP associated with activation of the TN-C promoter.

1. Morphology

Figure 2 shows representative phase contrast images of NIH 3T3 fibroblasts on films of collagen fibrils prepared at an alkanethiolate monolayer and at PS, and cells in the absence of collagen on PS and TCPS. As seen in Fig. 2, cells on collagen fibrils formed either on alkanethiolate monolayers or on PS have similar morphologies in that they are poorly spread. In contrast, on TCPS, and to a lesser extent on PS, in the absence of collagen, fibroblasts are more spread out, exhibiting lamellapodia and distinct leading and trailing edges.

While these cells adhere and spread moderately on PS in the absence of collagen as seen in Fig. 2(c), their response on PS treated with collagen is distinct. We used automated microscopy to compare these differences by quantifying the area to which cells spread on thin films of collagen on al-

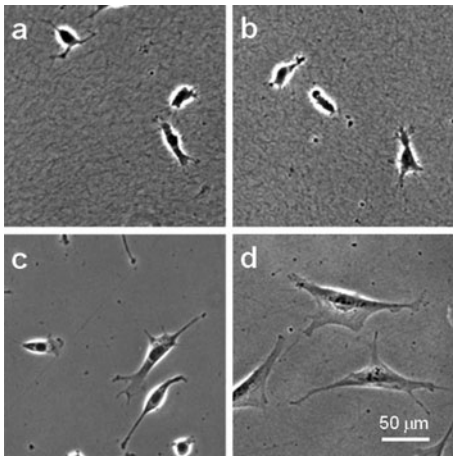

FIG. 2. Morphology of NIH 3T3 fibroblasts on different materials. Phase contrast images of cells on (a) collagen fibrils assembled at an alkanethiolate monolayer, (b) collagen fibrils assembled at PS, (c) untreated PS in the absence of collagen, and (d) TCPS.

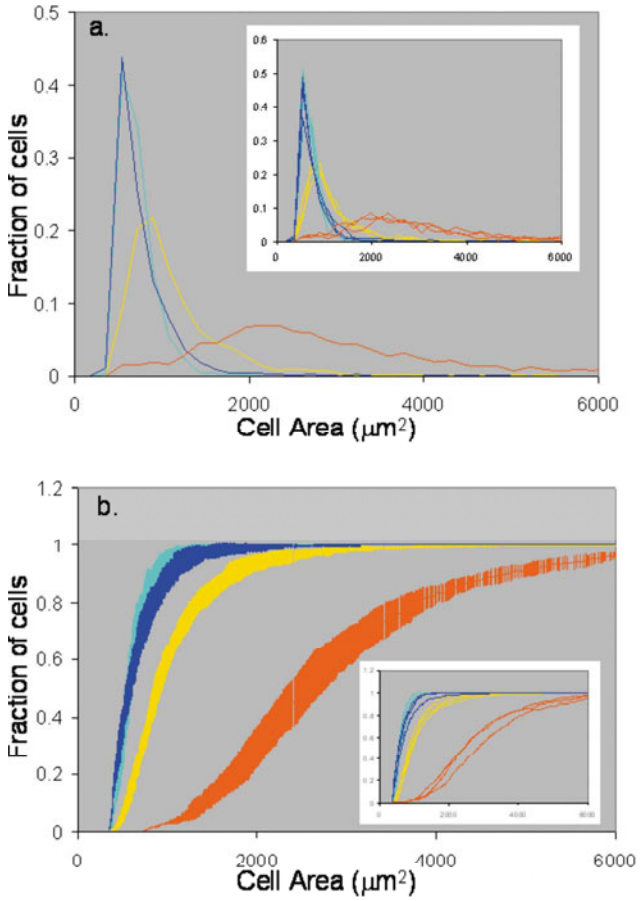

FIG. 3. Quantitative analysis of cell areas on different materials. (a) Histogram plot of cell areas measured across the population on each surface. Collagen fibrils on alkanethiolate monolayers, turquoise; collagen fibrils on PS, blue; untreated PS in the absence of collagen, yellow; TCPS, red. Inset shows the three replicates for each surface treatment. (b) Mean cumulative probability distributions and standard deviation bars of cell area for each surface. Inset shows each cumulative distribution for the three replicates of each surface treatment.

kanethiol and on PS with their response on TCPS and PS in the absence of collagen. The measurement of cell spread area relies on a combination of efficient cell staining and validated image analysis routines.[19] Between 130 and 500 cells with single nuclei were analyzed on each substrate, and three replicate substrates were analyzed for each material. Spread areas of cells under the different conditions are shown in two ways in Fig. 3, as histograms and as cumulative distribution plots. In Fig. 3(a) the cell area data are clustered into bins where each bin corresponds to a range of areas, and these binned data are plotted against the relative number of cells within that range of spread areas. As is typically observed, a distribution of cell areas characterizes the response of the population to each matrix condition, and these distributions are highly reproducible. The inset in Fig. 3(a) shows three replicate experiments using each material, and the averages of the replicates are plotted in the main figure. Cells appear to spread most on TCPS, least on collagen fibrils assembled at PS or at alkanethiols, and to an intermediate extent on PS not exposed to collagen. The histograms for cell areas on collagen fibrils indicate that cell spreading is similar on the fibrillar collagen films whether the films are formed at alkanethiolate monolayers or on PS.

While it is visually apparent that there is a high degree of overlap of the histogram data for cells on collagen fibrils formed at alkanethiolate monolayers and collagen fibrils formed on PS [Fig. 3(a)], statistical comparison of the distributions can be made by analyzing the data as cumulative distributions [Fig. 3(b)]. The cumulative plot is a running sum of the fraction of cells in the population with areas of a designated magnitude or smaller. The cumulative plotting method eliminates the need to cluster values into bins and normalizes the frequency of occurrence of a particular magnitude or less as a fraction of the population. From the replicate cumulative distribution curves [shown in inset, Fig. 3(b)], an average cumulative distribution function for each treatment was determined as described in Sec. II. The curves in Fig. 3(b) represent the mean cumulative distribution functions and the corresponding standard deviations in cumulative occurrence as determined from the replicates. The curves for cell areas measured for collagen fibrils on alkanethiols and collagen fibrils on PS lie on top of one another and are clearly distinct from curves for TCPS and PS not treated with collagen.

Two cumulative plots can be quantitatively compared to one another by evaluating the maximum absolute vertical differences between the curves.[18] To compare one treatment to another, at each *X*-axis value (i.e., measured value) the absolute differences between corresponding *Y*-axis values were determined, and the largest difference was taken as representative of the difference between the two curves. This difference is equivalent to the *D*-statistic of the Kolmogorov-Smirnov statistical test.[17] The *between-treatment D*-statistics were determined between the mean cumulative plots of the data from any two surface treatments and are shown in the first data column of Table I. In addition, the *D*-statistics were determined for each replicate curve compared to its corre-

TABLE I. Statistical analysis of cell spread area in response to surface treatment. NS indicates that treatments are not significantly different from one another; S indicates treatments are significantly different.

Treatment a vs treatment b	*Between-treatment D*-statistic	SE_a	SE_b	Ratio[a]	Statistical significance[b]
a. Collagen on alkanethiol b. Collagen on untreated PS	**0.9**	0.09	0.06	0.84	NS
a. Collagen on alkanethiol b. Untreated PS	0.48	0.09	0.05	4.45	S
a. Collagen on alkanethiol b. TCPS	0.93	0.09	0.07	8.12	S
a. Collagen on untreated PS b. Untreated PS	0.43	0.06	0.05	5.19	S
a. Collagen on untreated PS b. TCPS	0.90	0.06	0.07	9.80	S
a. TCPS b. Untreated PS	0.72	0.07	0.05	8.40	NS

[a]Test statisticratio=$D/(\sqrt{SE_a^2+SE_b^2})$.
[b]S indicates the test statistic ratio is greater than 3.

sponding mean curve and, using Eqs. (2a) and (2b), were used to calculate a standard error in *D* for the replicate measurements; we refer to these as *within-treatment D*-statistics. These standard errors (SEs) are listed in the second and third columns in Table I and correspond to each treatment of the pairs of treatments being compared.

It can be seen from Table I that the *between-treatment D*-statistic is relatively small (~0.1) when comparing cell areas on collagen assembled at alkanethiolate monolayers with collagen assembled on PS, indicating that differences between these data distributions are small. The *between-treatment D*-statistic is largest (~0.9) when comparing cells on collagen assembled at either alkanethiol or PS with TCPS, indicating the greatest differences in cell spread areas between these treatments. The *between-treatment D*-statistics for comparison of collagen treated surfaces with PS not treated with collagen is intermediate in value (~0.4).

We consider a difference between two treatments to be statistically significant if the *between-treatment D*-statistic is at least three times the value of the combined standard errors (SEs) in the replicates of the two treatments being compared. The combined standard errors are a measure of the *within-treatment D*-statistics. Table I shows the *between-treatment D*-statistics, the SEs for the treatments being compared, and the calculated test statistic ratios. Table I shows that the distribution of spread areas for cells on collagen films formed at alkanethiols and collagen films on PS were not significantly different from one another.

2. Tenascin-C promoter activity

For further comparison of cell response on collagen fibrils formed at PS with fibrils formed at alkanethiol surfaces, we examined activation of the promoter for the extracellular matrix protein, tenascin-C (TN-C). Expression of TN-C is modulated by the ECM composition[14,15,20] and by ECM mechanical properties.[4,21,22] TN-C expression is down-regulated in cells on collagen fibrils[14,15,23] or otherwise under treatments that inhibit cell division or prevent spreading.[6] So that the TN-C response of cells could be easily observed on the different substrates, stable transfectants (designated as TN-C-dsEGFP) were prepared using a DNA construct consisting of the TN-C gene promoter fused to the sequence for dsEGFP.[15] Figure 4 shows representative fluorescence images of cells on the different matrices to illustrate the relative activation of the promoter for the extracellular matrix protein, tenascin-C (TN-C) in cells on the different substrates. As seen in Fig. 4, compared to the cells on TCPS and PS in the absence of collagen, expression of GFP linked to the promoter for TN-C is weak on substrates of collagen fibrils, whether they are formed on alkanethiolate monolayers or PS.

The intensity of GFP was quantified in 130 to 500 cells on each matrix, and Fig. 5 shows the histogram and cumulative

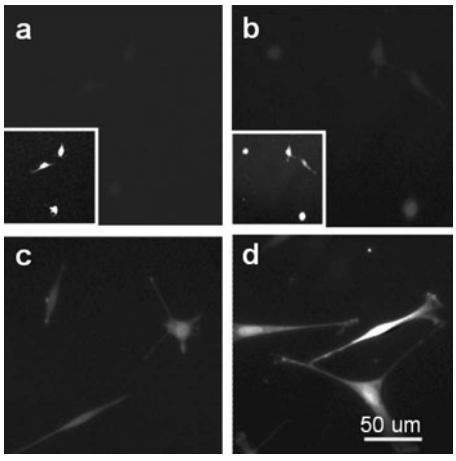

FIG. 4. TN-C-dsEGFP expression in NIH 3T3 fibroblasts on different materials. Fields were selected with automated stage positioning. Excitation and emission filters were 470/40 and 525/50 nm, respectively. GFP signal integration times for all fields in all experiments were 3 s. Contrast settings are identical for all images, except insets in (a) and (b), where contrast settings were increased sufficiently to allow visualization of cells. GFP fluorescence of cells on (a) collagen fibrils assembled at an alkanethiolate monolayer, (b) collagen fibrils assembled at PS, (c) untreated PS in the absence of collagen, and (d) TCPS.

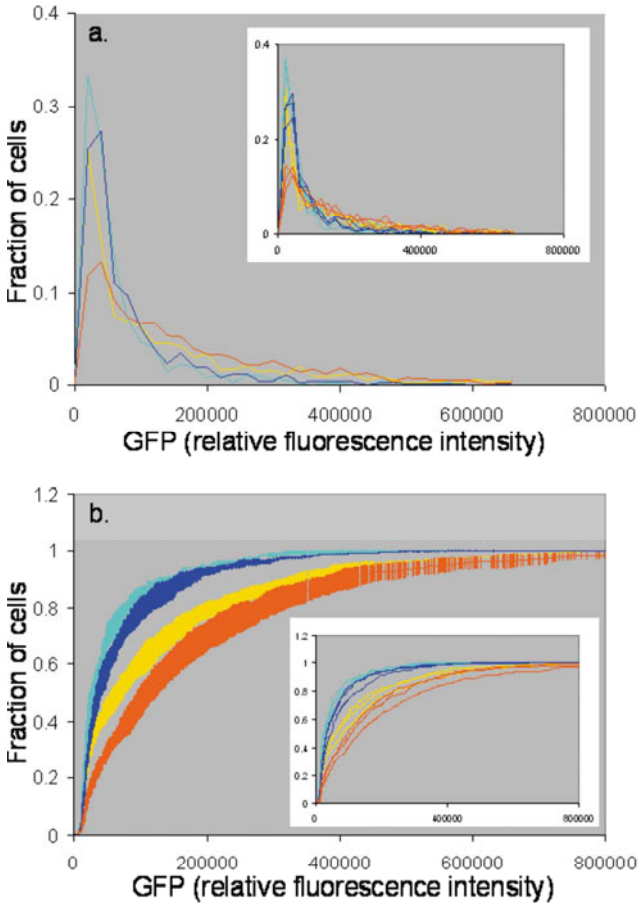

FIG. 5. Quantitative analysis of cell GFP intensities on different materials. (a) Histogram plot of relative GFP intensity measured across the population of cells on each surface. Collagen fibrils on alkanethiolate monolayers, turquoise; collagen fibrils on PS, blue; untreated PS in the absence of collagen, yellow; TCPS, red. Inset shows the three replicates for each surface treatment. (b) Mean cumulative probability distributions and standard deviation bars of cell area for each surface. Inset shows each cumulative distribution for the three replicates of each surface treatment.

plots of the expression of GFP in cells on the different substrates. The histogram plots [Fig. 5(a)] show that regardless of culture matrix, there is always a fraction of cells within each population that exhibits a relatively low level of fluorescence, which is equal to the intensity of autofluorescence observed in non-transfected cells. Compared to the cells on collagen films, the fraction of the population displaying a fluorescence signal less than 100 000 relative fluorescence intensity units decreases when cells are on untreated PS and decreases even more when they are on TCPS, and this decrease is accompanied by a corresponding increase in the number of cells that show higher levels of fluorescence. The histogram plots show that the number of cells expressing higher levels of GFP is greater in cells on TCPS and on untreated PS in the absence of collagen than on collagen fibrils. The wide variation in GFP intensities across the population and the extent of overlap between the histograms makes differences between the populations difficult to visualize until the data are plotted as cumulative distributions [Fig. 5(b)]. In these plots, the fraction of cells on TCPS and untreated PS with higher levels of GFP than cells on collagen-coated untreated PS and alkanethiolate monolayers can be clearly observed.

Analysis of the cumulative data for TN-C-dsEGFP expression is shown in Table II. The magnitude of the *between-treatment D*-statistic for the comparison of cells on fibrillar type 1 collagen assembled at PS or alkanethiols is small ($\sim$0.12) relative to the value determined for the comparison of either of the collagen treated surfaces to TCPS ($\sim$0.4) or PS ($\sim$0.3) in the absence of collagen. Again, the *D*-statistic is greatest when comparing cells on TCPS with cells on collagen fibrils, regardless of whether the fibrils were assembled at PS or alkanethiols. Using the criteria for statistical significance described above, the statistical test ratio indicates that the distribution of GFP expression levels in cells on collagen fibrils formed at alkanethiols or at PS are not statistically different. Thus it appears that both cellular responses, cell spread area and cellular TN-C promoter activity, are equiva-

TABLE II. Statistical analysis of TN-C promoter activity in response to surface treatment. NS indicates that treatments are not significantly different from one another; S indicates treatments are significantly different.

Treatment a vs treatment b	*Between-treatment D*-statistic	SE_a	SE_b	Ratio[a]	Statistical significance[b]
a. Collagen on alkanethiol b. Collagen on untreated PS	**0.12**	0.06	0.04	1.55	NS
a. Collagen on alkanethiol b. Untreated PS	0.26	0.06	0.05	3.21	S
a. Collagen on alkanethiol b. TCPS	0.48	0.06	0.04	5.20	S
a. Collagen on untreated PS b. Untreated PS	0.19	0.04	0.05	3.1	S
a. Collagen on untreated PS b. TCPS	0.33	0.04	0.04	5.63	S
a. TCPS b. Untreated PS	0.17	0.04	0.05	2.43	NS

[a]Test statistic ratio=$D/(\sqrt{SE_a^2+SE_b^2})$.
[b]S indicates test statistic ratio is greater than 3.

lent for cells on these two preparations of collagen fibrils.

IV. DISCUSSION

We have compared PS to self-assembled alkanethiolate monolayers on gold as substrates for supporting the formation of physiologically relevant collagen fibrils using several criteria: the physical supramolecular structure of the collagen fibrils formed, and two criteria of cell response, cell spread area and activation of the TN-C promoter. By these criteria, PS compares favorably to alkanethiolate monolayers as a substrate for forming thin films of type 1 collagen fibrils that can be used in cell culture experiments. We quantified the comparison of cell response by use of the *D*-statistic, which is a metric of the distance between the response distributions that resulted from different surface treatments.[18] This metric is useful because it takes into account changes that may occur over the entire distribution of cell responses but may not be adequately represented by a change in the mean value of the distribution. The statistical evaluation procedure described here takes into account the experimental error inherent in automated microscopy procedures and other cell-by-cell analysis techniques (e.g., flow cytometry).

The supramolecular structure of collagen has a strong effect on a number of phenotypic characteristics of cells. Various cell types have been reported to respond differently to fibrillar versus nonfibrillar collagen with respect to cell spreading.[9,15,24] The β1 integrin binding specificity for both nonfibrillar and fibrillar collagen[14,25] provides evidence for the role of the supramolecular structure of the collagen as critical to eliciting cell response. The role of the mechanical properties of the collagen fibrils in determining cell spreading has been implicated by observing greater cell spreading on stiffened collagen fibrils.[12] Also attributed to the supramolecular structure of collagen are reported differences in phosphorylation of ERK1/2,[14] changes in expression of a large number of genes including that of TN-C,[4,23] and retardation of cell cycle progression.[7,25] TN-C gene expression has also been shown to be dependent on collagen mechanical properties[4,21,22] and to involve complex intracellular pathways that are often associated with cell spreading and proliferation including MEK, ERK1/2 phosphorylation, and Rho A and ROCK activity.[6,26] Three distinct promoter regions have been identified in the full length TN-C promoter used in this study: a matrix response element associated with integrin engagement, a strain response element associated with response to the mechanical environment, and a serum response element.[26] By measuring both cell spreading and TN-C gene expression in cells, we are assessing a complex response to extracellular matrix presentation. It is very significant that response of cells as defined by these two markers is statistically equivalent in cells on collagen associated with PS or with alkanethiolate monolayers. It suggests that physiochemical features of fibrillar collagen present on the PS substrate are equivalent to those present on the collagen-treated alkanethiolate monolayer. It is also significant that the criteria for comparison of cell response to the two substrates involved examining the population distribution of responses and not simply a mean value, which would be much less sensitive to subtle differences.

Previously, we have shown that the cell response for both A10 vascular smooth muscle cells[9,11,14] and NIH 3T3 fibroblast cells[15] to fibrillar collagen films is nearly identical to their response to bulk fibrillar collagen gels and significantly different from the response observed on TCPS. Cells on TCPS are well-spread and have large proliferation rates while the cells on the fibrillar collagen films and collagen gels exhibit a more compact morphology and are growth arrested. The effects of the ECM on important intracellular events such as cytoskeleton regulation and proliferation make it clear why an appropriate ECM that is characterized and reproducible is essential when studying complex cell responses in applications such as drug discovery and systems biology. The thin films of fibrillar collagen presented here can serve as a convenient cell culture substrate that presents physiological relevant ECM signals to adherent cells.

A distinct advantage of fibrillar collagen films is the high degree of spatial homogeneity, which improves analysis by assuring that all cells within an experiment are exposed to the same ECM environment. This feature of collagen films also enables quantitation from a large numbers of cells by minimizing large changes in the focal plane during automated microscopy. In addition, lower levels of light scatter and fluorescence background compared to thick gels of collagen reduce ambiguity in quantitative fluorescence measurements of cells. While gold films on glass provide a better optical material than PS dishes in terms of lower light scatter, physical thickness of the substrate material, and better optical resolution, the convenience of PS makes this a desirable material on which to assemble thin films of type 1 collagen fibrils.

V. CONCLUSION

The results shown here indicate that films of fibrillar type 1 collagen can be formed on untreated polystyrene dishes. Cell response on these films, based on quantitative determination of morphology and TN-C promoter activity in NIH 3T3 fibroblasts, is statistically equivalent to cell response on collagen thin films on alkanethiolate monolayers. The use of films of collagen on PS should facilitate the preparation and reproducibility of biomimetic matrices for drug screening, maintaining cell phenotype, mechanistic studies, and intracellular pathway determinations, and may represent a first step toward standardized extracellular matrix surfaces. This study shows that films of type 1 collagen, with the advantages and characteristics of collagen films prepared at alkanethiolate surfaces, should be accessible to any high-content screening or cell biology laboratory.

ACKNOWLEDGMENTS

The authors would like to thank Charles Hagwood and Zhan-Qian Lu for discussions about the statistical procedures employed in this manuscript.

[1]M. E. Nimni, *Collagen* (CRC, Boca Raton, FL, 1988).
[2]C. J. Koh and A. Atala, J. Am. Soc. Nephrol. **15**, 1113 (2004).
[3]A. Boskey and C. N. Pleshko, Biomaterials **28**, 2465 (2007).
[4]D. Kessler, S. Dethlefsen, I. Haase, M. Plomann, F. Hirche, T. Krieg, and B. Eckes, J. Biol. Chem. **276**, 36575 (2001).
[5]C. D. Franco, G. Hou, and M. P. Bendeck, Trends Cardiovasc. Med. **12**, 143 (2002).
[6]R. Chapados, K. Abe, K. Ihida-Stansbury, D. McKean, A. T. Gates, M. Kern, S. Merklinger, J. Elliott, A. Plant, H. Shimokawa, and P. L. Jones, Circ. Res. **99**, 837 (2006).
[7]H. Koyama, E. W. Raines, K. E. Bornfeldt, J. M. Roberts, and R. Ross, Cell **87**, 1069 (1996).
[8]S. J. Wall, Z. D. Zhong, and Y. A. Declerck, J. Biol. Chem. **282**, 24471 (2007).
[9]J. T. Elliott, A. Tona, J. T. Woodward, P. L. Jones, and A. L. Plant, Langmuir **19**, 1506 (2003).
[10]M. Mrksich, Cell. Mol. Life Sci. **54**, 653 (1998).
[11]J. T. Elliott, J. T. Woodward, A. Umarji, Y. Mei, and A. Tona, Biomaterials **28**, 576 (2007).
[12]D. P. McDaniel, G. A. Shaw, J. T. Elliott, K. Bhadriraju, C. Meuse, K. H. Chung, and A. L. Plant, Biophys. J. **92**, 1759 (2007).
[13]F. Amyot, A. Small, H. Boukari, D. Sackett, J. Elliott, D. McDaniel, A. Plant, and A. Gandjbakhche, J. Biomed. Mat. Res. Part B (in press).
[14]J. T. Elliott, J. T. Woodward, K. J. Langenbach, A. Tona, P. L. Jones, and A. L. Plant, Matrix Biol. **24**, 489 (2005).
[15]K. J. Langenbach, J. T. Elliott, A. Tona, D. McDaniel, and A. L. Plant, BMC Biotechnol. **6**, 14 (2006).
[16]A. L. Plant, J. T. Elliott, A. Tona, D. McDaniel, and K. J. Langenbach, Methods Mol. Biol. **356**, 95 (2007).
[17]W. H. Press, S. A. Teukolsky, W. T. Vetterling, and B. P. Flannery, in *Numerical Recipies in C: The art of scientific computing*, 2nd ed., edited by W. T. Vetterling and B. P. Flannery (Cambridge University Press, Cambridge, England, 1992), p. 623.
[18]Z. E. Perlman, M. D. Slack, Y. Feng, T. J. Mitchison, L. F. Wu, and S. J. Altschuler, Science **306**, 1194 (2004).
[19]J. T. Elliott, A. Tona, and A. L. Plant, Cytometry A **52A**, 90 (2003).
[20]P. L. Jones and M. Rabinovitch, Circ. Res. **79**, 1131 (1996).
[21]M. Chiquet, A. S. Renedo, F. Huber, and M. Fluck, Matrix Biol. **22**, 73 (2003).
[22]T. W. Gilbert, A. M. Stewart-Akers, J. Sydeski, T. D. Nguyen, S. F. Badylak, and S. L. Woo, Tissue Eng. **13**, 1313 (2007).
[23]T. Ichii, H. Koyama, S. Tanaka, S. Kim, A. Shioi, Y. Okuno, E. W. Raines, H. Iwao, S. Otani, and Y. Nishizawa, Circ. Res. **88**, 460 (2001).
[24]I. Mercier, J. P. Lechaire, A. Desmouliere, F. Gaill, and M. Aumailley, Exp. Cell Res. **225**, 245 (1996).
[25]P. Henriet, Z. D. Zhong, P. C. Brooks, K. I. Weinberg, and Y. A. Declerck, Proc. Natl. Acad. Sci. U.S.A. **97**, 10026 (2000).
[26]P. L. Jones, F. S. Jones, B. Zhou, and M. Rabinovitch, J. Cell Sci. **112**, 435 (1999).